Heliyon 9 (2023) e16282

Contents lists available at ScienceDirect

Heliyon

journal homepage: www.cell.com/heliyon

Research article

Prediction of prognostic factors in breast cancer: A noninvasive method utilizing histogram parameters derived from Adc maps

Özge Tanişman [a,*], Fatma Tuba Kiziltepe [b], Çiğdem Yildirim [c], Zehra Sumru Coşar [b]

[a] Deparment of Radiology, Oltu State Hospital, Erzurum, Turkey
[b] Deparment of Radiology, University of Health Sciences Dr. Abdurrahman Yurtaslan Ankara Oncology Training and Research Hospital, Ankara, Turkey
[c] Department of Pathology, University of Health Sciences Dr. Abdurrahman Yurtaslan Ankara Oncology Training and Research Hospital, Ankara, Turkey

ARTICLE INFO

Keywords:
Breast imaging
Histogram analysis
Breast cancer
Magnetic resonance imaging

ABSTRACT

Objective: The aim of this study is to investigate the relationship between histogram parameters and prognostic factors of breast cancer and to reveal the diagnostic performance of histogram parameters in predicting prognostic factors status.

Materials and methods: Ninety-two patients with a confirmed histopathological diagnosis of breast cancer were included in the study. Magnetic resonance imaging (MRI) was performed using a 1.5T scanner and two different b values were used for diffusion-weighted imaging (DWI) (b values: 0 s/mm^2, b: 800 s/mm^2). For 3D histogram analysis, regions of interest (ROI) were drawn each slice of the lesion on apparent diffusion coefficient (ADC) maps. The following data were derived from the histogram analysis data: percentiles, skewness, kurtosis, and entropy. The relationship between prognostic factors and histogram analysis data was investigated using the Kolmogorov–Smirnov test, Shapiro–Wilk test, skewness-kurtosis test, independent *t*-test, Mann–Whitney *U* test, and Kruskal–Wallis test. Receiver operator characteristic (ROC) curve analysis was performed to evaluate the diagnostic performance of the histogram parameters.

Results: ADC_{max}, kurtosis, and entropy parameters were statistically significantly correlated with tumor diameter ($p = 0.002$, $p = 0.008$, and $p = 0.001$, respectively). There was a significant difference in $ADC_{90\%}$ and ADC_{max} values, depending on estrogen receptor (ER) and progesterone receptor (PR) status. These values were lower in ER- and PR-positive than ER- and PR-negative patients ($p = 0.02$ and $p = 0.001$ vs. $p = 0.018$, $p = 0.008$). All ADC percentage values were lower in patients with a positive Ki-67 proliferation index as compared with those with a negative Ki-67 proliferation index (all $p = 0.001$). The entropy value was high in high-grade lesions and lesions with axillary involvement ($p = 0.039$ and $p = 0.048$, respectively). The highest area under the curve (AUC) for ER and PR status was calculated for the $ADC_{90\%}$ value with ROC curve analysis. The highest AUC for Ki-67 proliferation index was found for the $ADC_{50\%}$.

Conclusion: Histogram analysis parameters derived from of ADC maps of whole lesions can reflect histopathological features of the tumors. Based on our study, it was concluded that histogram analysis parameters were related to the prognostic factors of the tumor.

* Corresponding author.
E-mail address: tanismanozge@gmail.com (Ö. Tanişman).

https://doi.org/10.1016/j.heliyon.2023.e16282
Received 3 November 2022; Received in revised form 4 May 2023; Accepted 11 May 2023
Available online 16 May 2023

1. Introduction

Breast cancer is a heterogeneous disease in which tumor histology, treatment response, and prognosis differ [1]. Tumor diameter, axillary lymph node involvement, histological grade, human epidermal growth factor receptor 2 (HER-2) expression, and hormone receptor status are prognostic markers in breast cancer [2]. The status of these prognostic markers plays a key role in treatment selection, prognosis determination and disease management. Many recent studies have investigated whether radiological images, specifically diffusion weighted imaging (DWI), reflect histological features of tissues. DWI, together with apparent diffusion coefficient (ADC) maps, can provide information about tissue cellularity. Some studies have investigated the relationship between breast cancer prognostic factors and ADC values. However, a consensus has yet to be reached regarding predicting prognostic factor of breast carcinoma for ADC maps. It has come to the fore that the histogram analysis of an ADC map can be used to determine the prognostic factors as it can provide more detailed information.

Histogram analysis is a statistical method that allows a detailed evaluation of radiological images. In whole lesion histogram analysis, signal intensities in a whole image are subjected to a statistical evaluation according to the values of each voxel in the radiological image. This method reveals not only the value of each voxel in the image but also the distribution and diversity of voxel values. The parameters derived from histogram analysis are percentile ADC values, skewness, kurtosis, and entropy. The histogram parameters of this study are as follows: minimum (min), 10th percentile, 25th percentile, 50th percentile, 75th percentile, 90th percentile, maximum (max), skewness, kurtosis, and entropy. The min represented the lowest value in the image, and the max represented the highest value. Percentiles means that percentage of pixels in the image and the highest numerical value for that percentage. For example, in the histogram analysis of an ADC image, if the value of $ADC_{25\%}$ is 1.5, it means that 25% of the pixels in the image have a value of between 0 and 1.49. Skewness, kurtosis, and entropy parameters obtained from histogram analysis reflect the distribution of pixel values in an image. Skewness has a negative value if values accumulate on the right of the mean and a positive value if values accumulate on the left. Positive skewness is recorded when most of the pixels in an image have values lower than the mean ADC value. Conversely, negative skewness is recorded when most of the pixels have values higher than the mean ADC value. Kurtosis is a measure of the distribution of values and peak value in the distribution. Entropy is a measure of randomness or homogeneity in the distribution of pixel values in an image and reflects heterogeneity in an image [3]. As the entropy value increases, the randomness of the distribution also increases.

Most histogram analysis studies of breast lesions have been designed to differentiate between benign and malignant lesions [4–6], with these studies primarily using mean, median, and percentile values [7–10]. Although some recent studies have focused on skewness and kurtosis, only a few of these studies have attempted to interpret the clinical meaning of skewness, kurtosis, and percentiles [7–11]. Skewness, kurtosis, and entropy parameters obtained from whole lesion histogram analysis reflect the distribution of pixels in the image. The hypothesis of this study was that skewness, kurtosis, and entropy values can function as imaging biomarkers that reflect the internal structure, heterogeneity, and cellularity of tumors. The aims of this study were to investigate the relationship between histogram parameters and prognostic factors in breast cancer and to reveal the diagnostic performance of histogram parameters.

2. Materials and methods

2.1. Patients

This study was approved by the ethics committee of our hospital, and written informed consent was obtained from all patients. The records of 1,640 patients with a histopathologically proven diagnosis of breast cancer between January 2018 and February 2021 were reviewed. Of these 1,640 cases, the records of 180 patients who had undergone preoperative breast magnetic resonance imaging (MRI) were selected for review. The exclusion criteria were an inability to retrieve MR images from the picture archiving and communication system (PACS) ($n = 12$), poor quality ADC maps ($n = 6$), and preoperative MRI scans with 3T scanner ($n = 70$). Based on these exclusion criteria, 92 patients with a histopathologically proven diagnosis of breast cancer were included in the study. All the patients were females (age range: 22−72 years; mean age: 48 years).

2.2. MRI protocol

MRI was performed using a 1.5T MRI system (Signa Explorer; GE Healthcare, Milwaukee, WI, USA) with an 8-channel breast coil. In all cases, the scans were performed with the patient in the prone position. The MRI protocols included axial T1-weighted, axial T2 IDEAL, DWI, dynamic contrast-enhanced 3D LAVA VIBRANT Flex sequences, and subtraction images from dynamic series. The

Table 1
The parameters of MRI sequences.

	TR (ms)	TE (ms)	MATRIX SIZE	FOV (mm)	SKICE THIKNESS (mm)	INTERSLICE GAP (mm)
T1W	626	Min full	320 × 256	320	5	1.0
T2 IDEAL	4996	96	320 × 256	320	5	1.0
3D LAVA VIBRANT FLEX	6.8	Min full	320 × 320	320	2.4	1.0
DWI	7421	–	140 × 160	320	5	no interslice gap

parameters for the axial T1-weighted images, axial T2 IDEAL images, 3D LAVA VIBRANT Flex sequences and DWI images are shown in Table 1. Diffusion-weighted images, which formed the basis of our study, were taken before contrast medium administration. The DWI sequence was obtained using the spin echo single shot echoplanar technique in three planes (x, y, z), with two b values (b: 0 s/mm^2; b: 800 s/mm^2). ADC values were automatically derived from the diffusion-weighted MR images using a standard monoexponential fit, which is on the console of the MR device.

2.3. Image analysis

The patients underwent MRI scan before biopsy. All images of 92 lesions obtained from the 92 patients were accessed via the PACS. A review of images was done by one radiologists with 5 years experience in radiology. All lesions were assessed in the absence of information on molecular subtype or immunohistochemical properties. First, the greatest tumor diameter and lesion type (mass or non-mass) were evaluated using MRI criteria of the BI-RADS lexicon 5th edition. The tumors were categorized into three groups according to lesion size using the 8th edition of the TNM classification.

2.4. Histogram analysis

The lesion images were then transferred from the PACS to a PC in DICOM format for processing with software (FireVoxel, version 372A, New York University). In the uploaded images, the entire lesion was drawn ROIs on each slice of the ADC maps for 3D volumetric analysis, with reference to corresponding conventional and postcontrast sequences. While drawing, care was taken to include cystic necrotic areas. The ROI drawing was made just inside the lesion edge. Thus, the entire lesion was included in the drawing, and partial volume effects were avoided. Histogram analysis data were obtained after sagittal and coronal plane configuration of the lesion, which was drawn along successive sections using 3D ROIs [Fig. 1(A–F),2 (A-E)].

2.5. Histopathological analysis

A pathologist experienced in breast pathology reviewed the histopathological records. In the immunohistochemical evaluation of the pathological specimens, estrogen receptor (ER), progesterone receptor (PR), HER2, and Ki-67 proliferation index status were determined, in addition to lesion grade and axillary involvement. The Ki-67 proliferation index was accepted as positive for staining of 20% or higher and negative for staining below 20% [12]. The histological tumor grade was assessed using the criteria of Bloom and Richardson (Figs. 3 and 4).

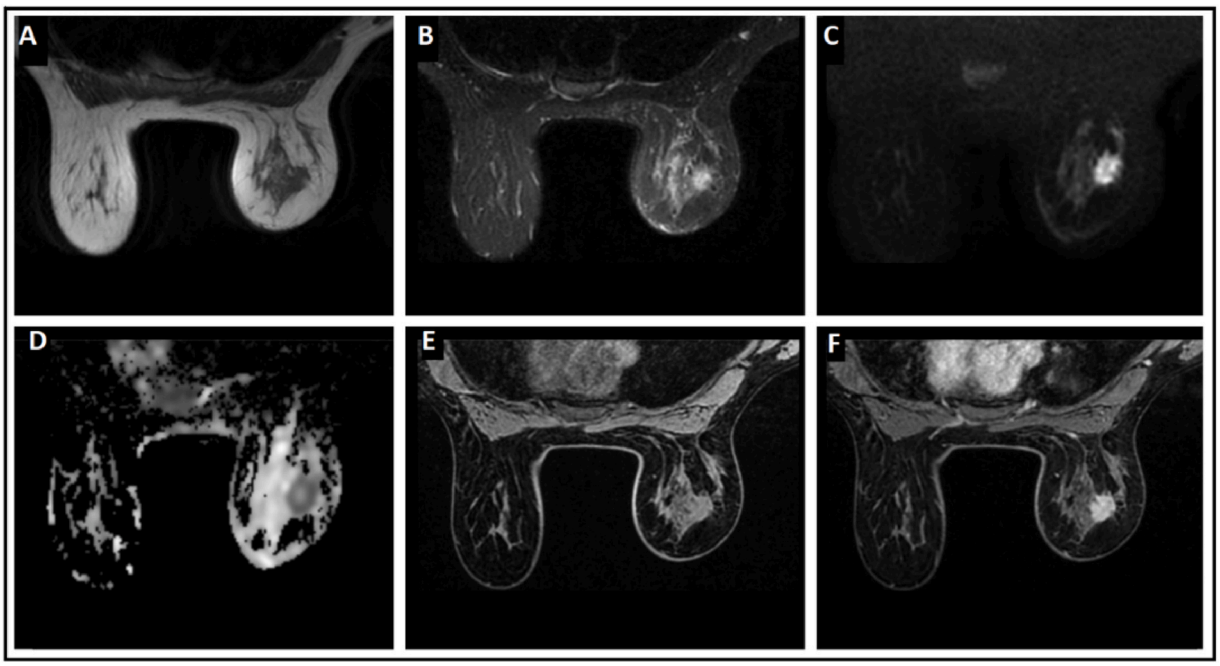

Fig. 1. 46-year-old woman with invasive ductal carcinoma in right breast. Spiculated contoured mass lesion in the upper outer quadrant on T1-weighted (A), fat-suppressed T2-weighted (B), b: 800 s/mm^2 DWI (C), ADC map (D), fat-suppressed precontrast T1-weighted (E), and fat-suppressed post-contrast T1-weighted (F) axial section MR images.

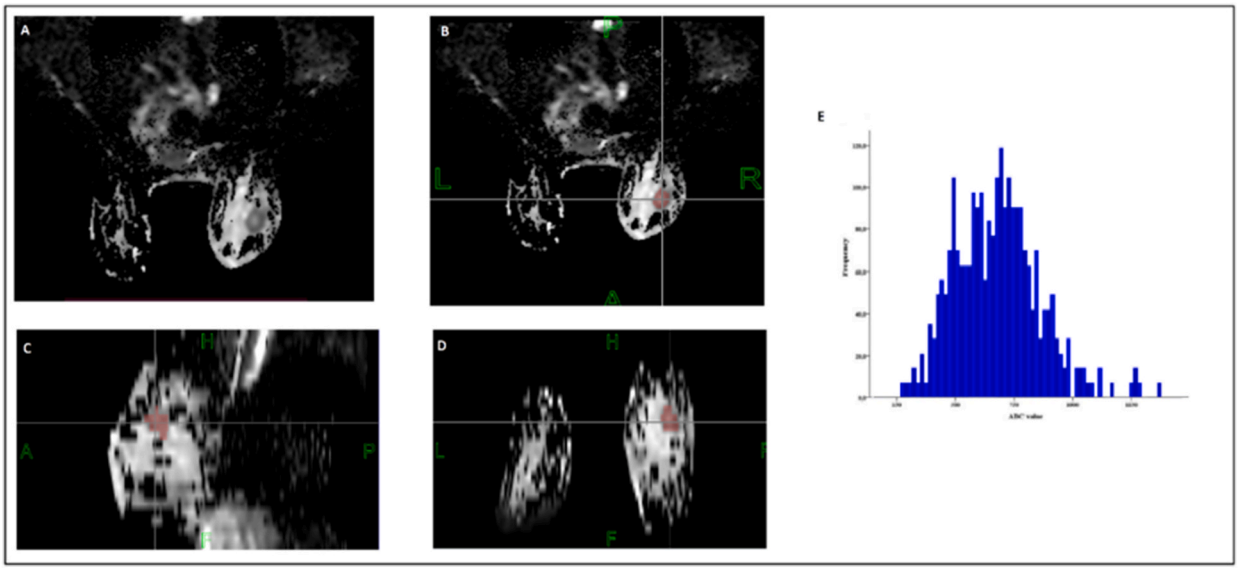

Fig. 2. ADC map of the lesion (A). 3D ROI image in the axial (B), sagittal (C), and coronal (D) planes in the ADC map for histogram analysis. ADC histogram based on entire lesion (E). Areas depicting high ADC and low ADC signals within the 3D ROI reflect the heterogeneity of the lesion. The entropy value was 3.69 and the lesion was grade 3. There was axillary involvement.

2.6. Statistical analysis

For data analysis, IBM SPSS Statistics, version 22.0 (IBM Corp., Armonk, NY) was used. Descriptive statistical methods (mean, standard deviation, median, frequency, ratio, minimum, and maximum) were used for evaluating the study data. Compliance of quantitative data with a normal distribution was tested by Kolmogorov–Smirnov, Shapiro–Wilk, and skewness-kurtosis tests. An independent *t*-test was used for comparisons of normally distributed quantitative data between two groups, and the Mann–Whitney *U* test was used for two-group comparisons of data that did not show a normal distribution. The Kruskal–Wallis test was used for comparisons of groups of three or more that did not show a normal distribution, and the Bonferroni Dunn test was used for pairwise comparisons. A level of $p < 0.05$ was considered statistically significant. Receiver operator characteristic (ROC) curve analysis was performed for assessing the diagnostic performance of the histogram parameters in distinguishing different immunohistochemical and pathological characteristics of breast cancer. Diagnostic screening tests (sensitivity, specificity, positive predictive value, and negative predictive value) and ROC curve analysis were used to determine the cut-offs for the parameters. A level of $p < 0.05$ was considered statistically significant.

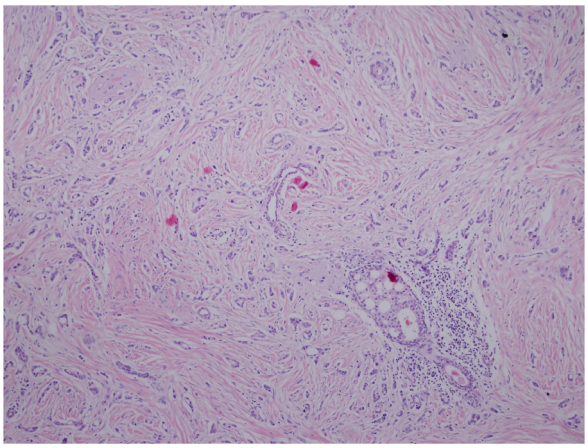

Fig. 3. — Histopathological evaluation of the same case. Sclerotic stroma shows infiltrative tumour developing as small tubular structures and thin cords. DCIS with cribriform morphology is observed in the right lower.

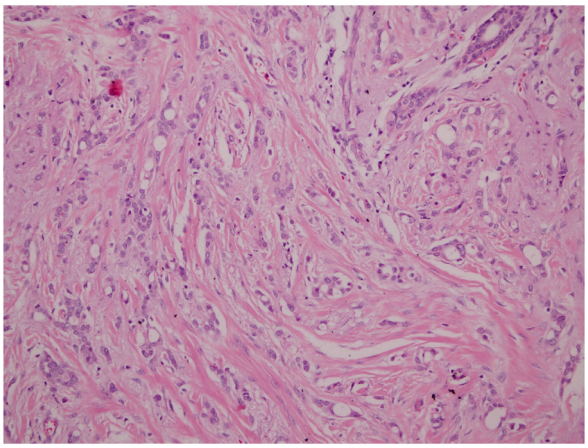

Fig. 4. H&E (x100): Large magnification shows pleomorphism, large nuclei and prominent nucleoli in the tumour cells. This lesion was grade 3.

3. Results

3.1. Characteristics of the tumors

In total, 92 lesions from patients with histopathologically proven invasive breast cancer were included in this study. Seventy-nine (85.9%) of the lesions were classified as mass, and 13 (14.1%) were classified as non-mass enhancement. The histopathological results of the patients are presented in Table 2.

3.2. Analysis of ADC histograms

The mean values for the histogram data of all the lesions were as follows: ADC_{min}: 0.7 (range: 0.3–1.1 – 10^{-3} mm^2/s); $ADC_{10\%}$: 0.84 (range: 0.3–1.3 × 10^{-3} mm^2/s); $ADC_{25\%}$: 0.92 (range: 0.4–1.4 × 10^{-3} mm^2/s); $ADC_{50\%}$: 1.01 (range: 0.5–1.5 × 10^{-3} mm^2/s); $ADC_{75\%}$: 1.11 (range: 0.7–1.6 × 10^{-3} mm^2/s); $ADC_{90\%}$: 1.2 (range: 0.7–1.7 × 10^{-3} mm^2/s), ADC_{max}: 1.46 (range: 0.9–1.9 × 10^{-3} mm^2/s); skewness: 2.78 (range: −8.6 to 9.9); kurtosis: −0.1 (range: −9.4 to 9.9); and entropy: 3.31 (range: −3.5 to4.8). A comparison of various ADC parameters in several subgroups defined by prognostic factors is summarized in Tables 3, 4.

When the histogram parameters of the two groups were compared according to lesion type (mass vs. non-mass enhancement), there was no statistically significant between-group difference, except for ADC_{max} measurements ($p > 0.05$). The ADC_{max} values for mass lesions were lower than those for non-mass enhancements ($p = 0.012$; $p < 0.05$).

The results revealed a statistically significant difference between the ADC_{max}, kurtosis and entropy measurements of the lesions according to tumor diameter ($p = 0.002$, $p = 0.008$ and $p = 0.001$, respectively; $p < 0.05$). There was no significant difference between other histogram parameters and tumor diameter ($p > 0.05$).

In paired comparisons for ADC_{max} measurements of those with a tumor diameter of 2–5 cm and ≥5 cm were higher than those with

Table 2
Prognostic features of the tumors.

		n	%
Tumor length (cm)	≤2 cm	29	31.5
	2–5 cm	55	59.8
	≥5 cm	8	8.7
ER	Negative	22	23.9
	Positive	70	76.1
PR	Negative	23	25.0
	Positive	69	75.0
HER-2	Negative	51	55.4
	+	18	19.6
	++	4	4.3
	+++	19	20.7
Ki-67 (%)	Negative	27	29.0
	Positive	65	71.0
Grade	1	10	10.8
	2	34	37.0
	3	48	52.2
AX	Negative	40	43.5
	Positive	52	56.5

Table 3
ADC histogram parameters according to prognostic factors.

Variables		No. of cases (%)	Mean (range)									
			ADC_{min} (10^{-3} mm^2/s)	$ADC_{10\%}$ (10^{-3} mm^2/s)	$ADC_{25\%}$ (10^{-3} mm^2/s)	$ADC_{50\%}$ (10^{-3} mm^2/s)	$ADC_{75\%}$ (10^{-3} mm^2/s)	$ADC_{90\%}$ (10^{-3} mm^2/s)	ADC_{max} (10^{-3} mm^2/s)	Skewness	Kurtosis	Entropy
Tumor size (mm)	≤20	29 (31)	0.75 (0.5/1.1)	0.84 (0.5/1.2)	0.91 (0.6/1.2)	1.01 (0.7/1.3)	1.11 (0.8/1.5)	1.19 (0.8/1.6)	1.33 (1/1.9)	1.44 (−8,6/9,9)	−2.58 (−9.4/5.3)	3.12 (1.6/3.9)
	20–50	55 (60)	0.68 (0.3/1)	0.83 (0.3/1.1)	0.91 (0.4/1.3)	1 (0.5/1.5)	1.1 (0.7/1.6)	1.2 (0.7/1.7)	1.5 (0.9/1.9)	3.53 (−5.9/9.7)	0.99 (−9.2/9.8)	3.42 (−3.5/4.3)
	>50	8 (9)	0.7 (0.4/1.1)	0.93 (0.6/1.3)	1.02 (0.7/1.4)	1.11 (0.8/1.5)	1.21 (0.8/1.5)	1.29 (0.9/1.6)	1.66 (1/1.9)	2.42 (−1.9/7)	1.42 (−8.7/9.9)	3.25 (0/4.8)
[b]*p* value			0.236	0.690	0.514	0.492	0.426	0.414	0.002**	0.124	0.008**	0.001**
Grade	1	10 (11)	0.75 (0.5/1.1)	0.88 (0.7/1.3)	0.95 (0.7/1.4)	1.04 (0.8/1.5)	1.11 (0.8/1.5)	1.17 (0.8/1.6)	1.36 (1/1.8)	0.90 (−6.4/9.7)	−1.04 (−6/5.3)	3.19 (1.6/4.1)
	2	34 (37)	0.69 (0.3/1.1)	0.82 (0.3/1.2)	0.90 (0.5/1.3)	1.00 (0.5/1.5)	1.10 (0.7/1.6)	1.19 (0.8/1.7)	1.42 (1/1.9)	2.29 (−5.9/9.6)	−0.88 (−9.4/9.9)	3.02 (−3.5/4.1)
	3	48 (52)	0.71 (0.3/1.1)	0.85 (0.4/1.3)	0.92 (0.4/1.3)	1.01 (0.5/1.4)	1.11 (0.7/1.5)	1.22 (0.7/1.6)	1.51 (0.9/1.9)	3.51 (−8.6/9.9)	0.64 (−8.4/9.8)	3.54 (1.4/4.8)
[b]*p* value			0.667	0.841	0.880	0.824	0.904	0.607	0.184	0.209	0.280	0.044*
Axillary involvement	Positive	52 (56.5)	0.69 (0.3/1.1)	0.83 (0.4/1.3)	0.91 (0.4/1.3)	1.00 (0.5/1.5)	1.10 (0.7/1.6)	1.19 (0.7/1.7)	1.47 (0.9/1.9)	2.99 (−8.6/9.9)	−0.01 (−9.4/9.8)	3.47 (0/4.8)
	Negative	40 (43.5)	0.73 (0.3/1.1)	0.85 (0.3/1.3)	0.93 (0.5/1.4)	1.02 (0.5/1.5)	1.12 (0.7/1.5)	1.22 (0.8/1.6)	1.45 (1/1.9)	2.50 (−5.2/9.7)	−0.22 (−9.2/9.9)	3.10 (−3.5/4.3)
p value			[c]0.302	[c]0.550	[c]0.586	[c]0.669	[c]0.652	[c]0.583	[c]0.701	[a]0.469	[a]0.741	[a]0.048

[a]Mann−Whitney *U* test, [b]Kruskal−Wallis test, independent samples *t*-test. *$p < 0.05$, **$p < 0.01$.

Table 4
ADC histogram parameters according to prognostic markers.

Variables		No. of cases (%)	Mean (range)									
			ADC_{min} (10^{-3} mm^2/s)	ADC_{10} (10^{-3} mm^2/s)	ADC_{25} (10^{-3} mm^2/s)	ADC_{50} (10^{-3} mm^2/s)	ADC_{75} (10^{-3} mm^2/s)	ADC_{90} (10^{-3} mm^2/s)	ADC_{max} (10^{-3} mm^2/s)	Skewness	Kurtosis	Entropy
ER	Positive	70 (76)	0.69 (0.3/1.1)	0.83 (0.3/1.3)	0.90 (0.4/1.4)	0.99 (0.5/1.5)	1.10 (0.7/1.6)	1.17 (0.7/1.7)	1.42 (0.9/1.9)	2.76 (−8,6/9,7)	−0.31 (−9.4/9.9)	3.42 (1.6/4.8)
	Negative	22 (24)	0.73 (0.4/1.1)	0.89 (0.6/1.3)	0.97 (0.7/1.3)	1.08 (0.9/1.4)	1.19 (0.9/1.5)	1.30 (1/1.6)	1.59 (1.1/1.9)	2.83 (−3.8/9.9)	0.56 (−8.4/9.8)	2.96 (−3.5/4.2)
p value			[c]0.378	[c]0.121	[c]0.069	[c]0.034*	[c]0.006**	[c]0.002**	[c]0.001**	[a]0.848	[a]0.528	[a]0.801
PR	Positive	23 (25)	0.70 (0.3/1.1)	0.86 (0.3/1.3)	0.90 (0.4/1.4)	0.99 (0.5/1.5)	1.09 (0.7/1.6)	1.18 (0.7/1.7)	1.42 (0.9/1.9)	2.77 (−8.6/9.7)	−0.35 (−9.4/9.9)	3.41 (1.6/4.8)
	Negative	69 (75)	0.72 (0.4/1.1)	0.88 (0.6/1.3)	0.96 (0.7/1.3)	1.07 (0.8/1.4)	1.17 (0.8/1.5)	1.28 (0.9/1.6)	1.57 (1.1/1.9)	2.80 (−3.8/9.9)	0.66 (−8.4/9.8)	3.00 (−3.5/4.2)
p value			[c]0.558	[c]0.212	[c]0.137	[c]0.081	[c]0.067	[c]0.018*	[c]0.008**	[a]0.818	[a]0.414	[a]0.950
HER-2	Positive	19 (21)	0.78 (0.4/1.1)	0.90 (0.6/1.3)	0.97 (0.7/1.3)	1.06 (0.8/1.4)	1.16 (0.9/1.4)	1.27 (1/1.6)	1.54 (1.2/1.9)	3.71 (−4.9/9.9)	0.33 (−9.4/8.1)	3.60 (2.9/4.2)
	Negative	73 (79)	0.69 (0.3/1.1)	0.83 (0.3/1.3)	0.90 (0.4/1.4)	1.00 (0.5/1.5)	1.09 (0.7/1.6)	1.19 (0.7/1.7)	1.44 (0.9/1.9)	2.54 (−8.6/9.7)	−0.21 (−8.7/9.9)	3.23 (−3.5/4.8)
p value			[c]0.054	[c]0.123	[c]0.140	[c]0.153	[c]0.082	[c]0.056	[c]0.071	[a]0.313	[a]0.415	[a]0.08
Kİ-67 (%)	<20	12 (13)	0.87 (0.6/1.1)	1.00 (0.7/1.3)	1.07 (0.8/1.4)	1.18 (0.9/1.5)	1.28 (0.9/1.6)	1.39 (1/1.7)	1.62 (1.1/1.9)	2.69 (−6.4/9.7)	0.09 (−8.1/9.8)	3.42 (1.4/4.1)
	≥20	80 (87)	0.63 (0.3/1)	0.78 (0.3/1)	0.85 (0.4/1.1)	0.94 (0.5/1.2)	1.04 (0.7/1.4)	1.13 (0.7/1.6)	1.39 (0.9/1.9)	2.81 (−8.6/9.9)	−0.18 (−9.4/9.9)	3.26 (−3.5/4.8)
p value			[c]0.001**	[c]0.001**	[c]0.001**	[c]0.001**	[c]0.001**	[c]0.001**	[c]0.001**	[a]0.976	[a]0.928	[a]0.574

[a]Mann−Whitney *U* test, [c]independent samples *t*-test, *$p < 0.05$, **$p < 0.01$.

a tumor diameter of ≤2 cm ($p = 0.030$ and $p = 0.005$, respectively; $p < 0.05$). No statistically significant difference was found between the ADC_{max} measurements of those with tumor diameters of 2–5 cm and ≥5 cm ($p > 0.05$).

In the comparisons between three groups, kurtosis measurements of lesions with diameters of 2–5 cm were higher than those with diameters of ≤2 cm ($p = 0.009$; $p < 0.01$). No significant difference was found in other paired comparisons for tumor diameter. ($p > 0.05$).

In the paired comparisons, the entropy values for tumors with diameters of 2–5 cm were higher than those for tumors with diameters of ≤2 cm ($p = 0.001$; $p < 0.01$). No significant difference was found in other pairwise comparisons for tumor diameter. ($p > 0.05$).

According to ER status, $ADC_{50\%}$, $ADC_{75\%}$, $ADC_{90\%}$, and ADC_{max} values were lower in the ER-positive group than in ER-negative group ($p = 0.034$, $p = 0.006$, $p = 0.002$, and $p = 0.001$, respectively; $p < 0.05$) (Fig. 5). There was no statistically significant difference in the ADC_{min}, $ADC_{10\%}$, $ADC_{25\%}$, skewness, kurtosis, and entropy measurements of the lesions according to ER status ($p > 0.05$). In terms of PR status, $ADC_{90\%}$ and ADC_{max} values in the PR-positive group were lower than those in the PR-negative group ($p = 0.018$ and $p = 0.008$, respectively; $p < 0.05$). When the PR-positive and PR-negative groups were compared, there was no statistically significant difference in ADC_{min}, $ADC_{10\%}$, $ADC_{25\%}$, $ADC_{50\%}$, $ADC_{75\%}$, skewness, kurtosis, and entropy measurements ($p > 0.05$).

Finally, in relation to HER2 status, there was no statistically significant difference between the HER-2 positive and HER-2 negative groups in any of the histogram analysis parameters evaluated.

According to the Ki-67 (%) index, there was a statistically significant difference in ADC_{min}, $ADC_{10\%}$, $ADC_{25\%}$, $ADC_{50\%}$, $ADC_{75\%}$, $ADC_{90\%}$, and ADC_{max} measurements of the lesions ($p = 0.001$ for all; $p < 0.05$). All these measurements were lower in Ki-67 (%) positive lesions than Ki-67 (%) negative lesions ($p = 0.001$; $p < 0.05$). There was no statistically significant difference in skewness, kurtosis, and entropy measurements ($p > 0.05$).

We found a statistically significant association between lesion grade and entropy measurements ($p = 0.044$; $p < 0.05$). In paired comparisons, entropy measurements of grade 3 lesions were higher than those of grade 2 lesions ($p = 0.039$; $p < 0.05$). There was no statistically significant difference in other paired comparisons for tumor grade. ($p > 0.05$). There was also no significant difference between grade and ADC_{min}, $ADC_{10\%}$, $ADC_{25\%}$, $ADC_{50\%}$, $ADC_{75\%}$, $ADC_{90\%}$, ADC_{max}, skewness, kurtosis values ($p > 0.05$).

Entropy values in lesions with axillary involvement were higher than those in lesions without involvement ($p = 0.048$; $p < 0.05$). There was no statistically significant difference in ADC_{min}, $ADC_{10\%}$, $ADC_{25\%}$, $ADC_{50\%}$, $ADC_{75\%}$, $ADC_{90\%}$, ADC_{max}, skewness, and kurtosis values according to axillary involvement ($p > 0.05$).

3.3. ROC curve analysis

Details on the diagnostic performance of the histogram parameters in distinguishing histopathological features of the tumors are provided in Table 5.

According to the ROC curve analyses, the $ADC_{90\%}$ value was the strongest parameter to distinguish between ER positive and ER negative (area under the curve [AUC]: 0.70). The optimum cut-off value was 1.25×10^{-3} mm^2/s (sensitivity: 67.14%; specificity: 68.18%). Lesions with an $ADC_{90\%}$ value of 1.25 or less were 4.37 times more likely to be ER positive (odds ratio [OR]: 4.37; 95% confidence interval [CI]: 1.56–12.22).

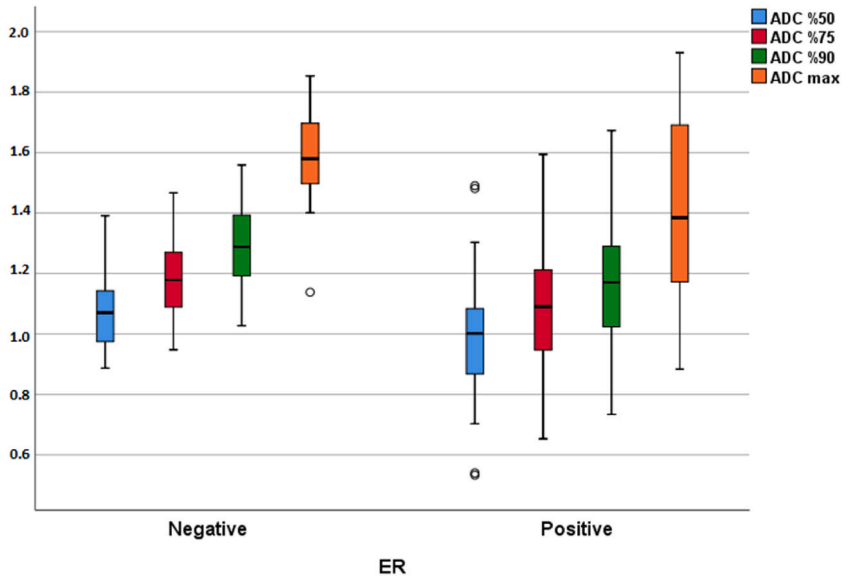

Fig. 5. — The box plot diagram for the results of the ER status. ADC50%, ADC75%, ADC90%, and ADCmax values were lower in the ERpositive group than in ER-negative group.

Table 5
Diagnostic performance of the histogram parameters in distinguishing histopathological features of the tumors.

Variables	Parameter	Diagnostic scan			ROC curve				
		Cut-off value	Sensitivity (%)	Specificity (%)	Positive predictive value	Negative predictive value	AUC	95% CI	*p*
ER	ADC_{50}	≤1.04	65.71	59.09	83.64	35.14	0.66	0.54–0.77	0.022*
	ADC_{75}	≤1.16	65.71	59.09	83.64	35.14	0.67	0.55–0.78	0.016*
	ADC_{90}	≤1.25	67.14	68.18	87.04	39.47	0.70	0.59–0.80	0.005**
	ADC_{max}	≤1.50	62.86	68.18	86.27	36.59	0.68	0.57–0.79	0.011*
PR	ADC_{90}	≤1.25	66.67	65.22	85.19	39.47	0.66	0.55–0.78	0.016*
	ADC_{max}	≤1.50	62.32	65.22	84.31	36.59	0.65	0.53–0.76	0.030*
Ki-67	ADC_{min}	≤0.81	93.85	77.78	90.04	84.00	0.88	0.80–0.96	0.001**
	ADC_{10}	≤0.94	92.31	77.78	90.91	80.77	0.88	0.79–0.97	0.001**
	ADC_{25}	≤0.98	84.62	77.78	90.16	67.74	0.87	0.78–0.96	0.001**
	ADC_{50}	≤1.07	86.15	77.78	90.32	70.00	0.89	0.81–0.96	0.001**
	ADC_{75}	≤1.18	86.15	74.07	88.89	68.97	0.87	0.79–0.95	0.001**
	ADC_{90}	≤1.29	89.23	70.37	87.88	73.08	0.85	0.76–0.94	0.001**
	ADC_{max}	≤1.57	73.85	66.67	84.21	51.43	0.75	0.64–0.87	0.001**
Grade	Entropy	≥3.4	72.92	54.55	63.64	64.86	0.64	0.53–0.76	0.016*
Axillary involvement	Entropy	≥3.4	71.15	55.00	67.27	59.46	0.62	0.50–0.73	0.048*

*$p < 0.05$, **$p < 0.01$.

In common with its role in predicting ER status, the $ADC_{90\%}$ had the highest AUC (0.66) for distinguishing between PR positive and PR negative (AUC: 0.66). The optimum cut-off value was 1.25×10^{-3} mm^2/s (sensitivity: 66.67%; specificity: 65.22%). Lesions with an $ADC_{90\%}$ value of 1.25 or below, the risk of PR positivity was 3.75 times higher (OR: 3.750; 95% CI: 1.38–10.12).

There was a statistically significant difference between Ki-67 status and all ADC percentile values (Fig. 6). Among the ADC values, the ADC50% value was the strongest parameter to predict Ki-67 positivity (AUC: 0.89; 95% CI: 0.81–0.96). The cut-off value for the $ADC_{50\%}$ value was 1.07×10^{-3} mm^2/s (sensitivity: 86.15%; specificity: 77.78%). The probability of a lesion being Ki-67 positive was 21.77 times higher in lesions with an $ADC_{50\%}$ value of 1.07 or below (OR: 21.77; 95% CI: 6.90–68.66).

The cut-off value for entropy was 3.4×10^{-3} mm^2/s to distinguish grade 3 lesions from grade 1 and 2 lesions (sensitivity: 72.92%; specificity: 54.55%). Lesions with an entropy value of 3.4 or higher were 3.23 times more likely to be grade 3 (OR: 3.23; 95% CI: 1.35–7.71).

The cut-off value for entropy in determining axillary involvement was 3.4×10^{-3} mm^2/s (sensitivity: 71.15%; specificity: 55.00%).

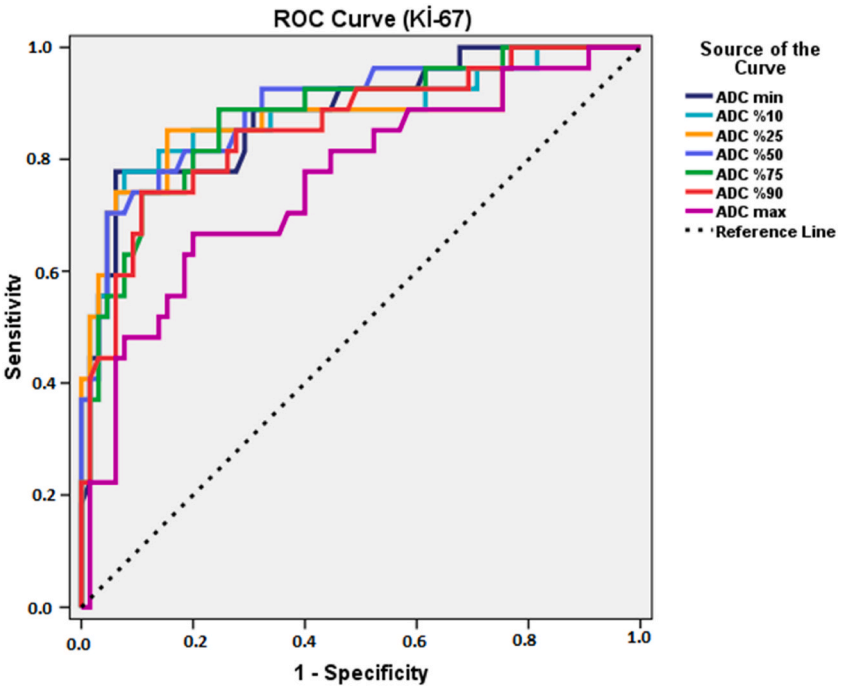

Fig. 6. ROC curves for ADC_{min}, $ADC_{10\%}$, $ADC_{25\%}$, $ADC_{50\%}$, $ADC_{75\%}$, $ADC_{90\%}$, and ADC_{max} levels according to the results of the Ki-67 proliferation index.

Lesions with an entropy value of 3.4 or higher were 3.01 times more likely to have positive axillary involvement (OR: 3.01; 95% CI: 1.27–7.15).

4. Discussion

The hypothesis of this study was that parameters of the ADC histogram analysis can function as imaging biomarkers that reflect the internal structure, heterogeneity, and cellularity of breast cancer tumors. To test this hypothesis, we investigated the relationship between prognostic factors associated with breast cancer tumors and histogram analysis parameters obtained from ADC maps. Our results revealed that a number of histogram parameters, such as percentiles, kurtosis, and entropy were associated with prognostic factors.

In the present study, when we compared the ADC_{max} values according to lesion type, the values of mass lesions were lower than those of non-mass enhancements ($p = 0.012$). Among all the parameters evaluated, only ADC_{max} differed significantly between the two groups (mass vs. non-mass enhancement). Kim et al. reported that percentile ADC values were higher in non-mass enhancements than in mass lesions, excluding ADC_{min} [2]. They attributed the higher ADC percentage values of non-mass lesions to the absence of a clear lesion boundary. As a result, measurements of these lesions include healthy parenchyma. The results of our study, unlike the literature, was only significant for ADC_{max} [2]. In our study, 29 (31.5%) of the 92 lesions were 2 cm or smaller, and the other 63 (68.5%) lesions were ≥2 cm. Necrosis and tumor heterogeneity increases in accordance with an increase in lesion size. Thus, the large number of lesions of ≥2 cm may explain our results.

Tumor size is an important prognostic factor. When we compared the ADC_{max} values of the tumor groups, those of lesions with diameters of 2–5 cm ($n = 55$) and ≥5 cm were higher than those of lesions with diameters of ≤2 cm ($p = 0.030$ and $p = 0.005$, respectively). Kim et al. reported that ADC values tended to be higher in lesions > 2 cm but reported a significant difference only for the $ADC_{10\%}$ value [2].

In our study, entropy and kurtosis values were higher in lesions with diameters of 2–5 cm than in lesions with diameters of ≤ 2 cm ($p = 0.001$ and $p = 0.008$, respectively). Kim et al. reported that tumors with diameters of >2 cm were associated with higher ADC kurtosis values than tumors with diameters of ≤2 cm [2]. Guan et al. reported higher ADC kurtosis values for cervical cancer lesions as compared with values for healthy cervical tissue [13]. Shindo et al. reported higher ADC kurtosis values in pancreatic adenocarcinomas compared to neuroendocrine tumors [14]. In both studies, high kurtosis values were associated with tumor heterogeneity [13,14]. To our knowledge, no studies have investigated the relationship between tumor diameter and ADC entropy values in breast cancer. As noted above, necrotic areas develop and tumor heterogeneity increases in accordance with an increase in lesion size. A high entropy value points to a random distribution pattern and heterogeneous signal intensity. In our study, the high rates of kurtosis and entropy in tumors with diameters of 2–5 cm were likely due to heterogeneity in the internal structures of the tumors.

ER and PR are nuclear transcription factors that regulate benign and malignant cell proliferation processes in breast tissue [15,16]. In our study, $ADC_{50\%}$, $ADC_{75\%}$, $ADC_{90\%}$, and ADC_{max} values in ER-positive patients were lower those than those in ER-negative patients ($p = 0.034$, $p = 0.006$, $p = 0.002$, and $p = 0.001$, respectively). Furthermore, $ADC_{90\%}$ and ADC_{max} values in the PR-positive group were lower than those in the PR-negative group ($p = 0.018$ and $p = 0.008$, respectively). Black et al. reported that cellularity was higher in ER-positive than ER-negative tumors [17]. However, Kim et al. found no correlation between ADC parameters and hormone receptor status in their histogram analysis study [2]. Choi et al. reported that $ADC_{25\%}$, $ADC_{50\%}$, and kurtosis values in ER-positive patients were lower than those in ER-negative patients [18]. As ERs and PRs are involved in the cell proliferation of breast tissue, cellularity is expected to be higher in hormone receptor positive tumors than hormone receptor negative tumors. The lower $ADC_{90\%}$ and ADC_{max} values in the ER-positive and PR-positive groups in our study as compared to those in the negative groups are associated with the higher cellularity of hormone receptor positive tumors. These findings are consistent with the literature.

HER-2 expression increases angiogenesis by inducing vascular endothelial growth factor [19–21]. We found no statistically significant difference in two groups (HER-2 positive vs HER-2 negative) in the parameters obtained from the histogram analysis ($p > 0.05$). It has been reported that HER-2 positive lesions have larger extracellular volume than HER-2 negative lesions and this may result in higher ADC values in HER- 2 positive group [2]. The fact that our results were different from the literature was associated with the presence of different tumor types in our study.

Ki-67 is a nuclear antigen that is expressed in the proliferation phase of the cell cycle [22]. In our study, all percentile ADC measurements obtained from the histogram were lower in the Ki-67 proliferation index positive group than in the negative group ($p = 0.001$). To our knowledge, no previous studies have investigated the association of the Ki-67 index with all ADC percentage values. Some previous studies found no relationship between the Ki-67 index and mean ADC value [23–25]. Others detected a weak relationship and concluded that the Ki-67 index cannot be used as a marker of proliferation activity [23–25]. In contrast, Kim et al. found that most ADC parameters in their histogram analysis were lower in those with a positive Ki-67 index than in those with negative Ki-67 index [2]. The results of our study are compatible with those of Kim et al. [2]. Based on our findings and those of Kim et al. [2], we conclude that measurements derived from whole lesions and evaluations of ADC maps with histogram analysis can provide additional information about the internal structure of tumors.

Tumor grade is a prognostic factor. Tumor grade is assessed according to tumoral cell differentiation and reflects both tumor aggressiveness and cellularity [2,26,27]. In our study, we detected no significant difference in ADC percentage values according to tumor grade ($p > 0.05$). However, in this study, entropy values in high-grade (grade 3) tumors were higher than those than in low-grade (grades 1 and 2) tumors ($p = 0.039$). To our knowledge, no studies have investigated the relationship between entropy and tumor grade. High entropy values indicate that the variability between voxel signal intensity forming the lesion is high. This shows the variation in signal intensity of the voxels forming the lesion. Based on the results of our study, we conclude that the entropy value in

ADC histogram analysis could be used as a radiological marker of tumor heterogeneity that can differentiate between high- and low-grade tumors.

The presence of axillary node metastasis and the size of the tumor are the two main prognostic factors used clinically [28]. In our study, entropy values were higher in lesions with axillary involvement than lesions without axillary involvement ($p = 0.048$). To our knowledge, no studies have investigated the relationship between axillary involvement and entropy or reported a positive correlation between these variables. In our study, the higher entropy values in the presence of axillary involvement were associated with tumor heterogeneity. Thus, we conclude that the entropy parameter of the histogram analysis could be used as a radiological marker in the evaluation of axillary involvement.

$ADC_{10\%}$ and $ADC_{25\%}$ parameters obtained from histogram analysis provide information about the signal intensity of 10% and 25% of the voxels in the examined area. In our study, $ADC_{10\%}$ and $ADC_{25\%}$ values were not associated with any prognostic factors, except the Ki-67 proliferation index. We thought that this finding may be related to the fact that the $ADC_{10\%}$ and $ADC_{25\%}$ parameters represent a small fraction of the lesions.

ROC analysis showed that $ADC_{90\%}$ relatively higher AUC for differentiating ER-positive and PR-positive from ER-negative and PR-negative with relatively high sensitivity and specificity. In determining the Ki-67 proliferation index, the highest AUC was calculated for the $ADC_{50\%}$ value. According to the ROC curve analysis, the cut-off value for entropy to distinguish tumor grade and axillary involvement was 3.4. The results of the present study did not reveal any one histogram parameter that can be used for all prognostic factors associated with breast cancer. The correlation of parameters of histogram analysis with prognostic factors in breast cancer suggest that radiological data can reflect the internal structures of tumors. To our knowledge, no previous studies related to ADC histogram parameters and prognostic factors of breast cancer have utilized ROC curves and cut-off values.

Our study has some limitations. First, the study was retrospective. Second, non-mass lesions were included in this study, which raise the possibility of including normal parenchyma in the measurements. Third, the study was based on images obtained using a 1.5T scanner and two different b values (0 and 800 s/mm^2). The use of multiple b values theoretically provides more accurate results. Fourth, a single radiologist evaluated all the radiological images, and interobserver variability was not studied. Fifth, due to the small number of patients in this study, multivariate analysis was not carried out. Sixth, since the necrotic component of the lesions was not assessed separately, the effect of necrosis on the results could not be detected. Finally, the lesion borders were drawn manually instead of using automatic segmentation. The latter may have limited standardization. Our results need to be supported by prospective studies, which are planned with a larger number of patients, measuring lesion borders by automatic segmentation and obtaining ADC maps with different parameters using multiple b values.

In conclusion, information on the histopathology of breast cancer lesions is the first step in the management of the disease. Based on our study, we conclude that prognostic factors can be predicted by evaluating ADC maps with histogram analysis. The finding of high entropy values in association with tumor heterogeneity is promising in terms of utilizing MRI, which is non-invasive method, to shed light on histopathological features of tumors.

Author contribution statement

ÖZGE TANİŞMAN: Conceived and designed the experiments; Performed the experiments; Analyzed and interpreted the data; Contributed reagents, materials, analysis tools or data; Wrote the paper.

Fatma Tuba KIZILTEPE: Conceived and designed the experiments; Analyzed and interpreted the data; Contributed reagents, materials, analysis tools or data.

Çiğdem YILDIRIM: Performed the experiments; Contributed reagents, materials, analysis tools or data.

Zehra Sumru COŞAR: Conceived and designed the experiments.

Data availability statement

Data included in article/supplementary material/referenced in article.

Declaration of competing interest

The authors declare that they have no known competing financial interests or personal relationships that could have appeared to influence the work reported in this paper.

References

[1] S.K. Jeh, S.H. Kim, H.S. Kim, et al., Correlation of the apparent diffusion coefficient value and dynamic magnetic resonance imaging findings with prognostic factors in invasive ductal carcinoma, Jan 33, J. Magn. Reson. Imag. (1) (2011) 102–109.

[2] E.J. Kim, S.H. Kim, G.E. Park, et al., Histogram analysis of apparent diffusion coefficient at 3.0t: correlation with prognostic factors and subtypes of invasive ductal carcinoma, J. Magn. Reson. Imag. 42 (6) (2015) 1666–1678.

[3] G. Castellano, L. Bonilha, L.M. Li, F. Cendes, Texture analysis of medical images, Dec, Clin. Radiol. 59 (12) (2004) 1061–1069.

[4] S. Suo, K. Zhang, M. Cao, et al., Characterization of breast masses as benign or malignant at 3.0T MRI with whole-lesion histogram analysis of the apparent diffusion coefficient, J. Magn. Reson. Imag. 43 (4) (2016) 894–902.

[5] H. Bougias, A. Ghiatas, D. Priovolos, K. Veliou, A. Christou, Radiography Whole-lesion histogram analysis metrics of the apparent diffusion coefficient as a marker of breast lesions characterization at 1 . 5 T, Radiography 23 (2) (2021) e41–e46.

[6] F. Xu, Y.Y. Liang, Y. Guo, et al., Diagnostic performance of whole-lesion apparent diffusion coefficient histogram analysis metrics for differentiating benign and malignant breast lesions: a systematic review and diagnostic meta-analysis, Sep. 1, Acta Radiol. 61 (9) (2020) 1–11.
[7] H.J. Baek, H.S. Kim, N. Kim, Y.J. Choi, Y.J. Kim, Percent change of perfusion skewness and kurtosis: a potential imaging biomarker for early treatment response in patients with newly diagnosed glioblastomas, Sep, Radiology 264 (3) (2012) 834–843.
[8] H. Chandarana, A.B. Rosenkrantz, T.C. Mussi, et al., Histogram analysis of whole-lesion enhancement in differentiating clear cell from papillary subtype of renal cell cancer, Dec, Radiology 265 (3) (2012) 790–798.
[9] K. Downey, S.F. Riches, V.A. Morgan, et al., Relationship between imaging biomarkers of stage i cervical cancer and poor-prognosis histologic features: quantitative histogram analysis of diffusion-weighted MR images, Feb, Am. J. Roentgenol. 200 (2) (2013) 314–320.
[10] A.D. King, K.K. Chow, K.H. Yu, et al., Head and neck squamous cell carcinoma: diagnostic performance of diffusion-weighted MR imaging for the prediction of treatment response, Feb, Radiology 266 (2) (2013) 531–538.
[11] N. Just, Improving tumour heterogeneity MRI assessment with histograms, Br. J. Cancer 111 (12) (2014) 2205–2213.
[12] J.V. Horvat, B. Bernard-Davila, T.H. Helbich, et al., Diffusion-weighted imaging (DWI) with apparent diffusion coefficient (ADC) mapping as a quantitative imaging biomarker for prediction of immunohistochemical receptor status, proliferation rate, and molecular subtypes of breast cancer, J. Magn. Reson. Imag. 50 (3) (2019) 836–846.
[13] Y. Guan, H. Shi, Y. Chen, et al., Whole-lesion histogram analysis of apparent diffusion coefficient for the assessment of cervical cancer, Mar, J. Comput. Assist. Tomogr. 40 (2) (2016) 212–217.
[14] T. Shindo, Y. Fukukura, T. Umanodan, et al., Histogram analysis of apparent diffusion coefficient in differentiating pancreatic adenocarcinoma and neuroendocrine tumor, Méd. 95 (4) (2016), e2574.
[15] S.R. Lakhani, I.O. Ellis, S.J. Schnitt, P.H.V.M. Tan van de, WHO Classification of Tumours of the Breast, fourth ed., IARC, Lyon, France, 2012.
[16] A.R. Daniel, C.R. Hagan, C.A. Lange, Progesterone receptor action: defining a role in breast cancer, Expet Rev. Endocrinol. Metabol. 6 (3) (2011) 359–369.
[17] R. Black, R. Prescott, K. Bers, A. Hawkins, H. Stewart, P. Forrest, Tumour cellularity, oestrogen receptors and prognosis in breast cancer (A), Clin. Oncol. Dec 9 (4) (1983) 311–318.
[18] Y. Choi, S.H. Kim, I.K. Youn, B.J. Kang, W.C. Park, A. Lee, Rim sign and histogram analysis of apparent diffusion coefficient values on diffusion-weighted MRI in triple-negative breast cancer: comparison with ER-positive subtype, PLoS One 12 (5) (2017) 1–12.
[19] F.J. Esteva, G.N. Hortobagyi, Prognostic molecular markers in early breast cancer, May, Breast Cancer Res. 6 (3) (2004) 109–118.
[20] E.A. Rakha, M.E. El-Sayed, A.R. Green, A.H.S. Lee, J.F. Robertson, I.O. Ellis, Prognostic markers in triple-negative breast cancer, Jan, Cancer 109 (1) (2007) 25–32.
[21] R. Kumar, The role of HER2 in angiogenesis, Oct 1, Semin. Oncol. 28 (2001) 27–32.
[22] H.K. Sung, S.C. Eun, S.K. Hyeon, et al., Diffusion-weighted imaging of breast cancer: correlation of the apparent diffusion coefficient value with prognostic factors, Sep, J. Magn. Reson. Imag. 30 (3) (2009) 615–620.
[23] A. Surov, P. Clauser, Y.W. Chang, et al., Can diffusion-weighted imaging predict tumor grade and expression of Ki-67 in breast cancer? A multicenter analysis, Jun, Breast Cancer Res. 20 (1) (2018) 1–7.
[24] S.-Y. Kim, E.-K. Kim, H.J. Moon, et al., Association among T2 signal intensity, necrosis, ADC and Ki-67 in estrogen receptor-positive and HER2-negative invasive ductal carcinoma, Magn. Reson. Imaging 54 (2018) 176–182.
[25] A. Surov, H.J. Meyer, A. Wienke, Associations between apparent diffusion coefficient (ADC) and KI 67 in different tumors: a meta-analysis. Part 1: ADC mean, Aug, Oncotarget 8 (43) (2017) 75434–75444.
[26] E.A. Rakha, J.S. Reis-Filho, F. Baehner, et al., Breast cancer prognostic classification in the molecular era: the role of histological grade, Aug, Breast Cancer Res. 12 (4) (2010) 207.
[27] C.W. Elston, I.O. Ellis, Pathological prognostic factors in breast cancer. I. The value of histological grade in breast cancer: experience from a large study with long-term follow-up, Nov, Histopathology 19 (5) (1991) 403–410.
[28] J.S. Ecanow, H. Abe, G.M. Newstead, D.B. Ecanow, J.M. Jeske, Axillary staging of breast cancer: what the radiologist should know, Oct, Radiographics 33 (6) (2013) 1589–1612.